Study of charge density distributions, elastic and inelastic electron scattering form factors and size radii for ^{19}F and ^{27}Al Nuclei

Zaid M. Abbas[1,2]* and Ghaith N. Flaiyh[1**]

[1]Department of Physics, College of Science, University of Baghdad, Baghdad- Iraq

[2]Department of Medical Physics, College of Science, Al-Nahrain University, Baghdad- Iraq

Abstract

Unitary Correlation Operator Method (UCOM) have been used to examine the ground state properties of ^{19}F and ^{27}Al nuclei such as, the charge densities, the root mean square (rms) radii, elastic electron scattering form factors. Inelastic longitudinal electron scattering form factors have been computed for isoscaler transition $T = 0$ of the ($0^+0 \rightarrow 2^+0$) and ($0^+0 \rightarrow 4^+0$) transitions for the ^{19}F and ^{27}Al nuclei. Discussion and comparison of the computed results with the obtainable experimental data have taken place. It was corroborative that the unitary correlation operator way is suitable to study the nuclear structure..

Keywords: Unitary Correlation Operator Method, Charge density distribution Elastic and Inelastic Form Factor.

PACS number: 21.10.Ft, 21.60.-n, 21.30.Fe

1.Introduction

Electron scattering is a particularly effective method for examining nuclear structure for stable nuclei. This is attributed the reality that electromagnetic interaction, which is comparatively low and famed — that is, electron dispersion is a ticklish inquiry to uncover the density distributions in nuclei — is how electrons interact with nuclei [1]. By using a candid unitary transformation, the UCOM was developed to characterize the main correlations brought about by the tensor interaction and short-range repulsion. For simple model spaces, the unitary transformation of the Hamiltonian results in a correlated interaction that is equivalent to a phase shift. [2]. A review in nuclear structure theory that tries to describe these interaction-induced correlations via unitary transformations was given by Roth et al. [3], their focus was the UCOM, which offers a very simple, comprehensive, and reliable way to correct short-range correlations. They discussed the UCOM formulation in considerable and highlighted its connexions to other ways of defining

these correlations and establishing effective interactions. The form factors F(q)'s were examined by Sharrad et al. [4] in order to account for distortion in nuclear collective modes in addition to the shell model transition density. By using the Tassie model's shape, the core polarization transition density was assessed. Mahmood and Flaiyh [5] investigated the form factors F (q) of inelastic longitudinal electron scattering. In addition to the shell model transition density, an equation for the transition charge density was examined. This transition charge density was utilized to compute the form factors for the ^{19}F and ^{27}Al nuclei. The core polarization transition density was assessed utilizing the form of the Tassie model and the consequent form of the ground state two-body charge density distributions (2BCDD's). Khilood et al. [6] used longitudinal form variables to calculate inelastic electron scattering. They investigated core polarization in longitudinal inelastic shell models and electron scattering shape variables. The current work aims to examine the influences of short-range central and tensor correlations on the ground state 2BCDD's, elastic and inelastic scattering form factors, and root mean square charge radii for ^{19}F and ^{27}Al nuclei.

2. Theoretical formulations

The operator is utilized to express the nucleon density of a nucleus composed of A point-such as particles: [7]

$$\hat{\rho}^{(1)}(\vec{r}) = \sum_{i=1}^{A} \delta(\vec{r} - \vec{r}_i) \quad (1)$$

to convert this operator for a two-body density taken as:

$$\sum_{i=1}^{A} \boldsymbol{\delta}(\vec{r} - \vec{r}_i) \equiv \frac{1}{2(A-1)} \sum_{i \neq j} \left\{ \boldsymbol{\delta}(\vec{r} - \vec{r}_i) + \boldsymbol{\delta}(\vec{r} - \vec{r}_j) \right\} \quad (2)$$

Actually, the two particles $\vec{r}_i$ and $\vec{r}_j$ coordinates , can really undergo a beneficial transformation that is in express of the relative $\vec{r}_{ij}$ and center of mass $\vec{R}_{ij}$ coordinates [8]:

$$\vec{r}_i = \frac{1}{\sqrt{2}} (\vec{R}_{ij} + \vec{r}_{ij}) \quad (3\text{-a})$$

$$\vec{r}_j = \frac{1}{\sqrt{2}} (\vec{R}_{ij} - \vec{r}_{ij}) \quad (3\text{-b})$$

Inserting eq's (3-a) and (3-b) to eq. (2) yields:

$$\hat{\rho}(2) \ (\vec{r}) = \frac{1}{2(A-1)} \sum_{i \neq j} \left\{ \delta \left[\vec{r} - \frac{1}{\sqrt{2}} (\vec{R}_{ij} + \vec{r}_{ij}) \right] + \delta \left[\vec{r} - \frac{1}{\sqrt{2}} (\vec{R}_{ij} - \vec{r}_{ij}) \right] \right\} \quad (4)$$

Using the identity:

$$\delta(a\vec{r}) = \frac{1}{|a^3|} \delta(\vec{r})$$

Where a is a constant, then eq. (4) becomes as:

$$\hat{\rho}(2)_{ch}(\vec{r}) = \frac{\sqrt{2}}{2(A-1)} \sum_{i\neq j} \left\{ \delta\left[\sqrt{2}\vec{r} - \vec{R}_{ij} - \vec{r}_{ij}\right] + \delta\left[\sqrt{2}\vec{r} - \vec{R}_{ij} + \vec{r}_{ij}\right] \right\} \quad (5)$$

Two-body correlation functions $\tilde{C}$ can generate a correlated two-body charge density operator as follows:

$$\hat{\rho}(2)_{corr}(\vec{r}) = \frac{\sqrt{2}}{2(A-1)} \sum_{i\neq j} \tilde{C} \left\{ \delta\left[\sqrt{2}\vec{r} - \vec{R}_{ij} - \vec{r}_{ij}\right] + \delta\left[\sqrt{2}\vec{r} - \vec{R}_{ij} + \vec{r}_{ij}\right] \right\} \tilde{C} \quad (6)$$

Where the correlation operator C is described as [3,9]:

$$C = C_{\Omega} C_r \quad (7)$$

Where C_r central correlations and C_{Ω} describes tensor correlations, each of these unitary operators are indicated by [9]:

$$C_r = \exp\left[-i \sum_{i<j} g_{r,ij}\right]$$

$$C_{\Omega} = \exp\left[-i \sum_{i<j} g_{\Omega,ij}\right] \quad (8)$$

The specifics of the generators g_r and g_{Ω} will rely on the particular NN interaction under account [9]. The generator for the central correlation is expressed as follows:

$$g_r = \sum_{S,T} \frac{1}{2} [q_r s_{ST}(r) + s_{ST}(r) q_r] \Pi_{ST} \quad (9)$$

Where Π_{ST} is the dropping operator onto two body spin S and isospin T. For two-body system could be computed using a numerically known correlation function $R_+(r)$. Thus, we parameterize the numerically specified $R_+(r)$ by [3,9]:

$$R_+(r) = r + \alpha \left(\frac{r}{\beta}\right)^{\eta} \exp\{-\exp(\frac{r}{\beta})\} \quad (10)$$

The parameter α is dominant the overall amount of the shift, β is the length scale, and η is determined the steepness around $r = 0$.

In a hermitized form, the complete generator for the tensor correlations is expressed as follows:

$$g_{\Omega} = \sum_T \vartheta_T(r) \; S_{12}(\vec{r}, \vec{q}_{\Omega}) \Pi_{1T} \quad (11)$$

Making use of the public definition for a rank 2 tensor operator:

$$S_{12}(\vec{a},\vec{b}) = \frac{3}{2}\left[(\vec{\sigma}_1.\vec{a})(\vec{\sigma}_2.\vec{b}) + (\vec{\sigma}_1.\vec{b})(\vec{\sigma}_2.\vec{a})\right] - \frac{1}{2}(\vec{\sigma}_1.\vec{\sigma}_2)(\vec{a}.\vec{b} + \vec{b}.\vec{a}) \quad (12)$$

The amplitude is presented by the tensor connection function $\vartheta_T(r)$. For $\vartheta_T(r)$ the next parameterization is utilized [3,9]:

$$\mathcal{G}_{(r)} = \alpha[1-\exp(-\frac{r}{\gamma})]\exp[-\exp(\frac{r}{\beta})] \quad (13)$$

The 2BCDD of nuclei is given by the expectation values of the associated two-body charge density operator of equation (6) and can be written as follows:

$$\rho_{ch}(r) = \langle \Psi \mid \hat{\rho}(2)_{corr.}(\vec{r}) \mid \Psi \rangle = \sum_{i\langle j} \langle i\, j \mid \hat{\rho}(2)_{corr.}(\vec{r}) \left[\mid ij \rangle - \mid ji \rangle \right] \quad (14)$$

Where the two particles wave function is utilized as [10]:

$$|ij\rangle = \sum_{JM_J}\sum_{TM_T} \left\langle j_i m_i\, j_j m_j \middle| JM_J \right\rangle \left\langle t_i m_{t_i}\, t_j m_{t_j} \middle| TM_T \right\rangle \left|(j_i j_j) JM_J\right\rangle \left|(t_i t_j) TM_T\right\rangle \quad (15)$$

Since our correlated two-body charge density operator of equation (6) is created in formulas of $\vec{r}_{ij}$ and $\vec{R}_{ij}$ coordinates, the space-spin portion $\left|(j_i j_j) JM_J\right\rangle$ of the two-particle wave function built in the jj-coupling scheme should be converted in idioms of these coordinates.

Defines the mean square charge radii of the nuclei under consideration as [7].

$$\left\langle r^2 \right\rangle = \frac{4\pi}{Z}\int_0^\infty \rho_{ch}(r)\, r^4 dr \quad (16)$$

Utilizing the ground-state charge density allocation (from equation 14), the elastic form factor should be examined. Since the fallen and dispersed electron waves are regarded as plane waves, the form factor in the Plane Wave Born Approximation is just the Fourier convert of CDD. As a result [11, 12]:

$$F(q) = \frac{4\pi}{Z}\int_0^\infty \rho_{ch}(r)\, j_0(qr) r^2 dr \quad (17)$$

Where $j_0(qr) = sin(qr)\ /(qr)$ is the 0^{th} order of the spherical Bessel function and q is the momentum transfer, eq. (17) that should be written as follows:

$$F(q) = \frac{4\pi}{qZ}\int_0^\infty \rho_{ch}(r)\, sin(\, qr)r \quad dr \tag{18}$$

Where $F_{fs}(q)$ is the correction for finite nucleon size and $F_{cm}(q)$ is the center of mass correction. These corrections take forms [13].

$$F_{fs}(q) = e^{-0.43q^2/4} \tag{19}$$

$$F_{cm}(q) = e^{q^2b^2/4A} \tag{20}$$

Inserting equation(19) and (20) into eq. (18), we get:

$$F(q) = \frac{4\pi}{qZ}\int_0^\infty \rho_{ch}(r)\, Sin(qr)r \quad drF_{fs}(q)F_{cm}(q) \tag{21}$$

Inelastic longitudinal form factors, including angular momentum J and q, may be idiom as follows [14].

$$\left|F_J^L(q)\right|^2 = \frac{4\pi}{Z^2(2J_i+1)}\left|\, \langle f \left\| \hat{T}_J^L(q) \right\| i\rangle \,\right|^2 |F_{cm}(q)|^2 \left|F_{fs}(q)\right|^2 \tag{22}$$

The longitudinal operator is acquainted as [13].

$$\hat{T}_{Jt_z}^L(q) = \int dr\; j_J(qr)\, Y_J(\Omega)\;\; \rho(r, t_z) \tag{23}$$

Where $\rho(r, t_z)$ is the charge density operator**.** With the configuration mixing, the reduced matrix elements in spin and isospin space of the longitudinal operator between the system's initial and final particle states are expressed as [13]:

$$\langle f \;\|\|\hat{T}_{JT}^L\;\|\|\; i\rangle = \sum_{a,b} OBDM^{JT}(i, f, J, a, b)\;\; \langle b \;\|\|\; \hat{T}_{JT}^L \;\|\|\; a\rangle \tag{24}$$

Where OBDM is the One Body Density Matrix elements are computed in formulas of the isospin–reduced matrix elements. The several particles reduced matrix elements of longitudinal operator are given as [13]:

$$\langle f \|\; \hat{T}_J^L(\tau_Z, q)\| i\rangle = \left\langle f \left\| \hat{T}_J^{ms}(\tau_Z, q) \right\| i \right\rangle + \left\langle f \left\| \hat{T}_J^{cor}(\tau_Z, q) \right\| i \right\rangle \tag{25}$$

Equation (25) provides the model space matrix element as follows:

$$\left\langle f \left\| \hat{T}_J^{ms}(\tau_Z, q) \right\| i \right\rangle = e_i \int_0^\infty dr r^2 j_J(qr) \overset{ms}{\rho}_{J,\tau_Z}(i, f, r) \tag{26}$$

The model space transition density $\overset{ms}{\rho}_J(i, f, r)$ is idiomed by [13]:

$$\rho_{J,\tau_z}^{ms}(i, f, r) = \sum_{jj'(ms)}^{ms} OBDM\;\; (i, f, J, j\,, j', \tau_z)\, \langle j||Y_J||j'\rangle\, R_{nl}(r)R_{n'l'}(r) \tag{27}$$

Equation (25) provides the core polarization matrix element is the ensuing form [11, 12].

$$\left\langle f \left|\right| \overset{cor}{\hat{T}_J^L}(\tau_z, q) \left|\right| i \right\rangle = e_i \int_0^\infty dr\, r^2 j_J(qr) \;\; \overset{core}{\rho}_J(i, f, r) \tag{28}$$

where $\overset{core}{\rho}_J$ is the core-polarization transition density (CP). So the overall transition density is:

$$\rho_{J\tau_z}(i,f,r) = \overset{ms}{\rho}_{J\tau_z}(i,f,r) + \overset{core}{\rho}_{J\tau_z}(i,f,r) \quad (29)$$

CP is written by Tassie shape [15].

$$\rho^{core}_{Jt_z}(i,f,r) = N\frac{1}{2}(1+\tau_z)r^{J-1}\frac{d\rho_o(i,f,r)}{dr} \quad (30)$$

Where ρ_o is the ground state 2BCDD and N is a proportional constant, is provided as [15]:

$$N = \frac{\int_0^\infty drr^{J+2}) \quad -\sqrt{(2J_i+1)B(CJ)}}{(2J+1)\int_0^\infty drr^{2J}\rho_o(i,f,r)} \quad (31)$$

Where B(CJ) is the reduced transition probability

3. Results and Discussion

For ^{19}F and ^{27}Al nuclei, the computations for the ground state 2BCDDs ($\rho_{ch}(r)$), the root mean square charge radii $\langle {r_{ch}}^2\rangle^{\frac{1}{2}}$, and the elastic and inelastic form factors $F(q)'s$ are performed. The higher state $1d_{5/2}$ and $2s_{1/2}$ are involved in the computations for nuclei. The occupation probabilities of higher state is presented in Table (1). The strong of the correlations are established by properly the computed $\langle {r_{ch}}^2\rangle^{\frac{1}{2}}$ with those of empirical data. The central and tensor parameters needed in the computations of $\langle {r_{ch}}^2\rangle^{\frac{1}{2}}$, $\rho_{ch}(r)$ and $F(q)'s$ are shown in Table (1) and Table (2). Besides, the calculated $\langle {r_{ch}}^2\rangle^{\frac{1}{2}}$ including the effect of UCOM are in very match approval with those of experimental data. Figure (1) illustrate the computed charge density distributions for ^{19}F [Fig.1(a)] and ^{27}Al [Fig. 1(b)] nuclei obtained by UCOM influence and without it, along with the fitted to the experiential data. We notice that the effect of UCOM influence showed improvement in the results to match the experimental data.

Table (1)

The parameters of Short-Range Central correlations which have been utilized in the current work's computations

Nuclei	Occupation percentage	b (fm)	α (fm)	β (fm)	η	$\langle {r_{ch}}^2\rangle^{\frac{1}{2}}$ (fm)	$\langle {r_{ch}}^2\rangle^{\frac{1}{2}}$ (fm) Exp. [16]

^{19}F	$1d_{5/2}$	0.0166	1.84	1.49	1.74	0.135	2.792027	2.8976
	$2s_{1/2}$	0.45						
^{27}Al	$\mathbf{1d_{5/2}}$	0.6333	1.92	1.81	2.06	0.015	3.074077	3.0610
	$\mathbf{2s_{1/2}}$	0.6						

Table (2)

Tensor correlations, the parameters utilized in the current work's computations

Channel	$\alpha\ (fm)$	$\beta\ (fm)$	γ
$S = 0, T = 1 even$	**1.81**	**1.07**	**0.67**
$S = 1, T = 0 even$	**1.43**	**0.95**	**0.78**
$S = 0, T = 0 odd$	**2.3**	**1.0**	**0.9**
$S = 1, T = 1 odd$			

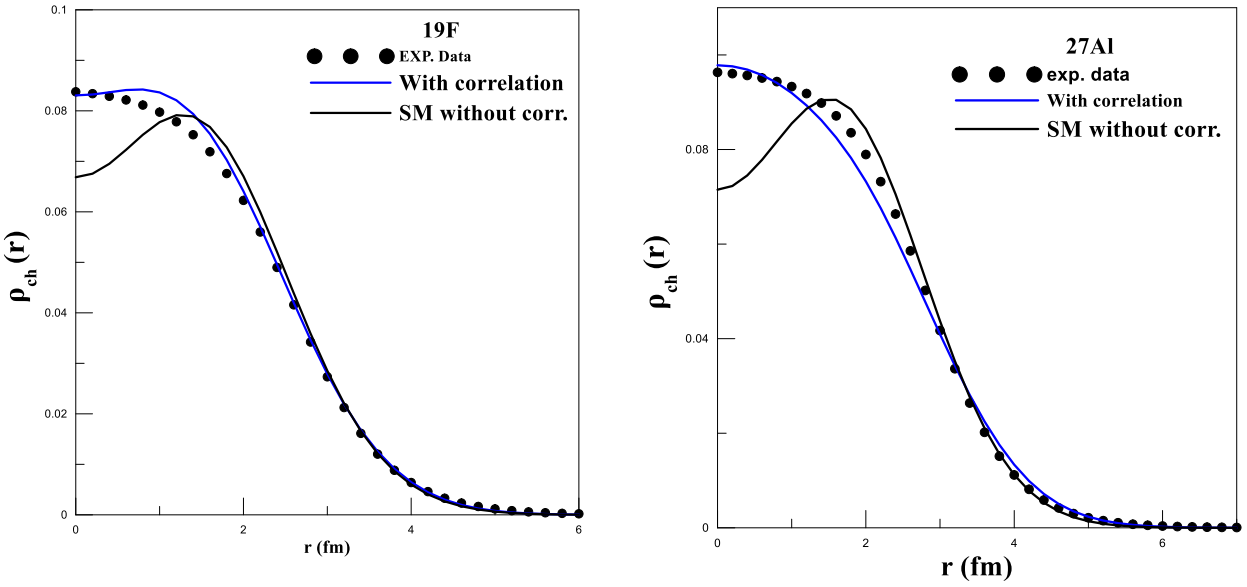

(a) **(b)**

Figure 1: Calculated charge density distribution for ^{19}F (Fig a) and ^{27}Al (Fig. b) nuclei with UCOM parameters compared with the experimental data [17].

The elastic form factors of ^{19}F and ^{27}Al nuclei are showed in Fig. (2.a) and (2.b), consecutively. It is notice from this figures that both of the value and attitude of the computed form factors are in credible approval with those of empirical data during the whole zone of q. In

addition, the places of the computed diffraction minima in both computations of curves are recreated. It is also observed that the addition of the UCOM influence to the red curve computations results in a minor improvement in the estimated form factor outcomes, as well as a slight amelioration in the magnitudes of the form factor in the momentum transfer zone.

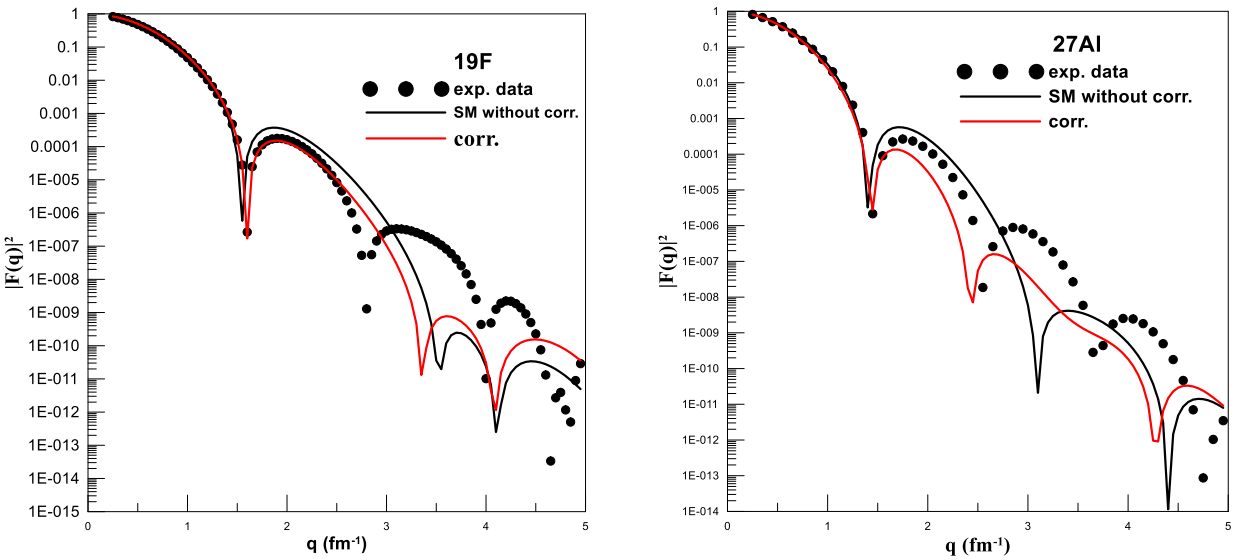

(a) **(b)**

Figure 2: Elastic Form Factor for ^{19}F (Fig. a) and ^{27}Al (Fig b) nuclei. The filled circle marks are experimental data [17].

The C2 form factors of ^{19}F and ^{27}Al nuclei are illustrated in figures 3(a) and 3(b) consecutively. The computed C2 form factors are planned as a function of the q for the transitions, $(J_i^\pi T_i \rightarrow J_f^\pi T_f)$,$0^+0 \rightarrow 2_1^+0$ (with an observed excitation energy of $E_x = 1554\, MeV$ [18] and $B(C2) = 35.32\, e^2.fm^4$ [19]) for ^{19}F and $0^+0 \rightarrow 2_1^+0$ (with an observed Ex=0.844 MeV [20] and $B(C2) = 12.79 \pm 0.5\, e^2.fm^4$) for ^{27}Al [21] . The model space MS contribution is illustrated by red curves when configuration mixing is included, and the core polarization CP contribution is showed by blue curves when two-body correlations are included. The entire contribution, which is derived by accounting for both the MS and CP, is displayed in these figures by black curves. The outcomes illustrate that adding the impact of CP to MS greatly improves

the results. Furthermore, the black curve, which depicts the combined effect, matches the experimental values extremely well.

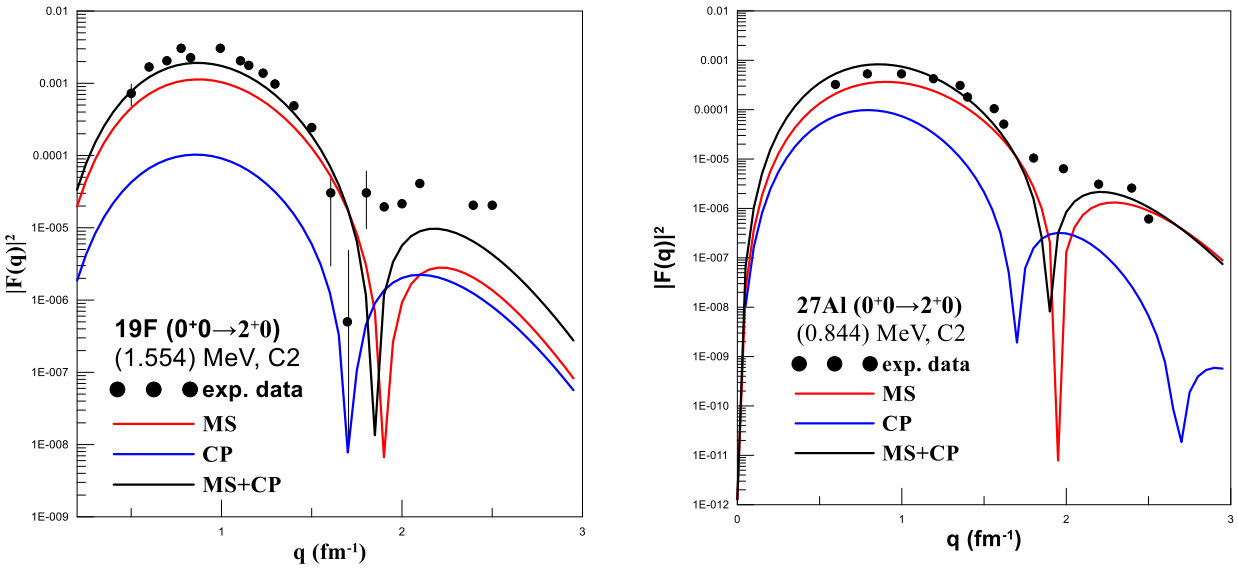

(a) **(b)**

Figure 3: The C2 form factors for ^{19}F (Fig. a) and ^{27}Al (Fig b) nuclei are compared with experimental data [22] and [23] consecutively.

The C4 form factor of ^{19}F nucleus is shown in figure 4. Here, the computed C4 form factor is planned as a function of the q for the transitions$\left(J_i^\pi T_i \rightarrow J_f^\pi T_f\right) = \left(\frac{5}{2}^+ \frac{1}{2} \rightarrow \frac{9}{2}^+ \frac{1}{2}\right)$ in ^{19}F with an excitation energy of $2.78\,MeV$ [24]. The *B(C4)* of the above nucleus is $4669\,e^2.fm^4$[19]. In this figure, the red curves show the referring of the MS when configuration mixing is included in consideration, and the blue curves show CP contribution when two-body correlations are factored into account. We notice that MS closely aligns with the empirical data. By adding the effect of CP, we get the solid black curve representing the total sum, which shows a good approval with the empirical values. However, when CP influence is introduced into MS, the results get to be in resonant accordance with the experimental datum across the entire ambit of q.

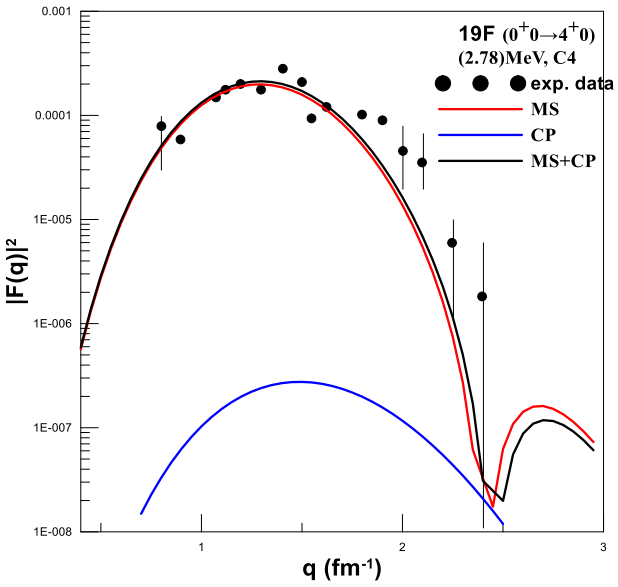

Figure 4: The C4 form factors for ^{19}F nucleus is compared with empirical data [22].

The nucleus of the ^{27}Al had been examined. Computation is offered for the transitions from the ground state at 2.211 MeV. The major quandary that prohibits the ^{27}Al nucleus from improving computations is the proximity of the first 4^+ 0 and second 2^+ 0 states, which have a very small experimental energy separation and, as it turns out, preclude electron scattering experiments to resolve them. The outcomes of $C2$ (blue curve), $C4$ (red curve) and the $C2 + C4$ (black curve) form factors for these states are offered in figure (5). Bearing in mind the influence of CP together with MS, ushering in a strengthening of the $C2 + C4$ form factors and therefore making the computed outcomes to be in suitable assent with the experiential data.

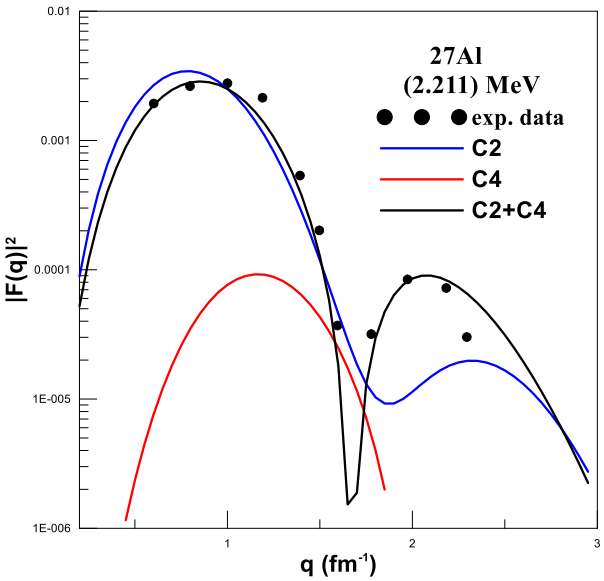

Figure 5: **The (C2+C4) form factors for ^{27}Al nucleus is compared with the experimental data [23].**

4. Conclusions

In the current research, by adding the UCOM to the 2BCDD's formula, we achieved an outstanding approval with the experimental outcomes for the $\rho_{ch}(r)$ and $\langle {r_{ch}}^2 \rangle^{\frac{1}{2}}$. Based on the $\rho_{ch}(r)$ used in the elastic form factor calculations, we achieved a match approval with the experimental outcomes. In the computation of inelastic form factors, and based on the $\rho_{ch}(r)$ to account for the effect of CP, we obtained results that match the experimental data. From computed results of the form factor, we observed that adding CP to MS significantly improves the results, ensuring alignment with experimental values. From the above observations, it is evident that utilizing the UCOM effect is highly effective in studying nuclear structure properties. This examination contributes to a better knowledge of ^{19}F and ^{27}Al nuclear structure, which is crucial for researching nuclear interactions.

References

[1] R. Srivastava and D. V. Fursa, Electron scattering from Atoms, Ions, and Molecules, Basel: MDPI, (2023).

[2] T. Neff and H. Feldmeier, Nucl. Phys. A713,311(2003). https://doi.org/10.1016/S0375-9474%2802%2901307-6

[3] Robert Roth, Thomas Neff, Hans Feldmeier; Prog. Part. Nucl. Phys. 65 (2010) 50 https://doi.org/10.1016/j.ppnp.2010.02.003.

[4] F.I. Sharrad, A.K. Hamoudi, R.A. Radhi and H.Y. Abdullah, J. Natn. Sci. Foundation Sri Lanka 2013 41 (3): 209-217. http://dx.doi.org/10.4038/jnsfsr.v41i3.6053

[5] R. I. Mahmood and G. N. Flaiyh, Iraqi Journal of Science, 2017, Vol. 58, No.3C, pp: 1660-1667. DOI: 10.24996/ ijs.2017.58.3C.9

[6] Khilood H. Ali1 and Khalid S. Jassim, Archs Sci. (2024) Volume 74, Issue 3 Pages 114-117. DOI: https://doi.org/10.62227/as/74319

[7] A. N. Antonov, P. E. Hodgson and I. Zh. Petkov, "Nucleon Momentum and Density Distribution in Nuclei", Clarendon Press, Oxford, (1988).

[8] N. Paar, P. Papakonstantinou, R. Roth, H. Hergert , Int. J. Mod. Phys. E15 (2006) 346-353. https://doi.org/10.1142/S0218301306004193

[9] H. Feldmeier, T. Neff, R. Roth, J. Schnack, Nucl.Phys. A632 (1998) 61-95**.** https://doi.org/10.1016/S0375-9474(97)00805-1

[10] Kris. L. G. Heyde, ‘'The Nuclear Shell Model", Springer-Verlag Berlin Heidelberg, (1994).

[11] H. G. Benson and B. H. Flowers; Nucl. Phys., A126, 305(1969). https://doi.org/10.1016/0375-9474(69)90469-2

[12] J. D. Walecka, "Electron Scattering for Nuclear and Nucleon Structure", Cambridge University Press, Cambridge, (2001).

[13] B. A. Brown, B. H. Wildenthal, C. F. Williamson, F. N.Rad, S. Kowalski, Hall Crannell and J. T. O'Brien; Phys. Rev., C32, 1127 (1985). https://doi.org/10.1103/PhysRevC.32.1127

[14] R.A. Radhi, A.A. Abdullah, A.H. Raheem; Nuclear Physics A 798 (2008) 16–28. https://doi.org/10.1016/j.nuclphysa.2007.10.010

[15] G. N. Flaiyh; Iraqi Journal of Physics, Vol. 13 No. 28 (2015). https://ijp.uobaghdad.edu.iq/index.php/physics/article/view/239

[16] I. Angeli, K. P. Marinova, Atomic Data and Nuclear Data tables, 99 (2013) 69-95. https://doi.org/10.1016/j.adt.2011.12.006

[17] H. De Vries, C. W. De Jager and C. DE Vries, Atomic Data and Nuclear Tables 36 (1987) 495-536. https://doi.org/10.1016/0092-640X(87)90013-1

[18] R. Yen, L. S. Cardman, D. Kalinsky, J. R. Legg, C. K. Bockelman; Nucl. Phys., **A235**,135, (1974). https://doi.org/10.1016/0375-9474(74)90182-1

[19] K. S. Jassim and S. R. Sahib; Journal of Chemical and Pharmaceutical Sciences, 10(2), (2017) 1070-1074. https://www.researchgate.net/publication/315735528

[20] Y. Horikawa, Y. Tovizuka and A. Nakada; Phys.Lett., **B39**, 9, (1971).

[21] G. C. Li, M. R. Yearian and I. Sick; Phys. Rev., **C9**, 1861, (1974). https://doi.org/10.1103/PhysRevC.9.1861

[22] T. W. Donnelly and I. Sick; Rev. Mod. Phys., 56, 461(1984). https://doi.org/10.1103/RevModPhys.56.461

[23] K. Whitner,C. Williamson and S. Kowalski; Phys. Rev.,C22, 374,(1980). https://doi.org/10.1103/PhysRevC.22.374

[24] Tilley D.R, Weller H.R, Cheves C.M and Chasteler R.M, Energy levels of light nuclei A= 19. Nuclear Physics A, 595, 1995, 1. https://doi.org/10.1016/0375-9474(95)00338-1